THE ASTROPHYSICAL JOURNAL, 493:222–229, 1998 January 20

THE DEFINITIVE ABUNDANCE OF INTERSTELLAR OXYGEN[1]

DAVID M. MEYER
Department of Physics and Astronomy, Northwestern University, Evanston, IL 60208; meyer@elvis.astro.nwu.edu
M. JURA
Department of Physics and Astronomy, University of California, Los Angeles, CA 90095-1562; jura@clotho.astro.ucla.edu
AND
JASON A. CARDELLI[2]
Department of Astronomy and Astrophysics, Villanova University, Villanova, PA 19085
Received 1997 July 11; accepted 1997 September 2

ABSTRACT

Using the Goddard High Resolution Spectrograph (GHRS) onboard the *Hubble Space Telescope*, we have obtained high signal-to-noise (S/N) ratio echelle observations of the weak interstellar O I λ1356 absorption toward the stars γ Cas, ϵ Per, δ Ori, ϵ Ori, 15 Mon, τ CMa, and γ Ara. In combination with previous GHRS measurements in six other sight lines (ζ Per, ξ Per, λ Ori, ι Ori, κ Ori, and ζ Oph), these new observations yield a mean interstellar gas-phase oxygen abundance (per 10^6 H atoms) of 10^6 O/H = 319 $\pm$ 14. The largest deviation from the mean is less than 18%, and there are no statistically significant variations in the measured O abundances from sight line to sight line and no evidence of density-dependent oxygen depletion from the gas phase. Assuming various mixtures of silicates and oxides, the abundance of interstellar oxygen tied up in dust grains is unlikely to surpass 10^6 O/H $\approx$ 180. Consequently, the GHRS observations imply that the *total* abundance of interstellar oxygen (gas plus grains) is homogeneous in the vicinity of the Sun and about two-thirds of the solar value of 10^6 O/H = 741 $\pm$ 130. This oxygen deficit is consistent with that observed in nearby B stars and similar to that recently found for interstellar krypton with GHRS. Possible explanations for this deficit include: (1) early solar system enrichment by a local supernova, (2) a recent infall of metal-poor gas in the local Milky Way, or (3) an outward diffusion of the Sun from a smaller Galactocentric distance.

Subject headings: ISM: abundances — ISM: atoms — ultraviolet: ISM

1. INTRODUCTION

Oxygen is the most abundant element in the Galaxy after hydrogen and helium. Consequently, it is important to establish accurately the current epoch O abundance for studies of Galactic chemical evolution (Timmes, Woosley, & Weaver 1995). A considerable effort has recently been made in determining the abundances of oxygen and other elements in nearby B stars, since these young stars should most closely reflect the current ISM abundance pattern (Gies & Lambert 1992; Kilian 1992; Cunha & Lambert 1994; Kilian, Montenbruck, & Nissen 1994). These studies yield a median B star oxygen abundance (per 10^6 H atoms) of 10^6 O/H $\approx$ 450, which is about two-thirds of the Grevesse & Noels (1993) solar value (10^6 O/H = 741 $\pm$ 130). This result is inconsistent with the traditional assumptions that the solar abundance reflects that of the ISM at the time of the Sun's formation 4.6 Gyr ago and that the interstellar O abundance should increase slowly over time (Audouze & Tinsley 1976; Timmes et al. 1995).

A simple interpretation of the conflict between the solar and B star abundances is that it is a manifestation of the abundance scatter in their respective stellar populations. For example, Cunha & Lambert (1994) find a spread of $\pm$0.2 dex among the oxygen abundances in their sample of Orion association B stars. Also, in a sample of F and G stars of age and Galactocentric radius similar to those of the Sun, Edvardsson et al. (1993) find an iron abundance spread of $\pm$0.25 dex, with the Sun among the most metal-rich cases. Such scatter in the stellar abundances is strongly suggestive of localized abundance inhomogeneities in the ISM. Yet, as discussed by Roy & Kunth (1995), a variety of hydrodynamical processes operating in the Galactic disk should keep the gas chemically well mixed on short timescales. In order to determine the homogeneity of the local interstellar medium at a level capable of distinguishing between a solar and a B star oxygen abundance, it is necessary to obtain very sensitive observations.

Since O I (13.618 eV) and H I (13.598 eV) have nearly the same ionization potentials, O I is the dominant form of gaseous oxygen in diffuse interstellar H I clouds. Although the prominent O I λ1302 absorption line is typically saturated in diffuse sight lines, the very weak intersystem transition at 1355.598 Å can yield accurate gas-phase O abundances if measured with sufficient sensitivity. Observations of this line with the *Copernicus* satellite indicate a mean interstellar gas-phase oxygen abundance that is 40%–70% of the solar value (York et al. 1983; Keenan, Hibbert, & Dufton 1985). However, the scatter in these data is too great to rule out a solar abundance of interstellar oxygen, especially since some of the O is tied up in dust grains. This scatter is primarily due to the uncertainties associated with measuring the weak O I λ1356 line strengths.

The ability of the GHRS on board the *Hubble Space Telescope* (*HST*) to obtain UV spectra with higher resolution and S/N ratios than those acquired with *Copernicus* has made it possible to take interstellar abundance studies another step forward with accurate observations of very weak absorption lines (Savage & Sembach 1996). Utilizing

[1] Based on observations obtained with the NASA/ESA *Hubble Space Telescope* through the Space Telescope Science Institute, which is operated by the Association of Universities for Research in Astronomy, Inc., under NASA contract NASA-26555.
[2] Deceased 1996 May 14.

high-S/N GHRS observations of the O I λ1356 absorption in the low-density sight lines toward the stars ι Ori and κ Ori, Meyer et al. (1994) have found a total oxygen abundance (gas plus grains) in Orion that is consistent with the stellar (Cunha & Lambert 1994) and nebular determinations (Baldwin et al. 1991; Rubin et al. 1991; Osterbrock, Tran, & Veilleux 1992; Peimbert, Storey, & Torres-Peimbert 1993). In this paper, we present new O I λ1356 data; our total GHRS sample includes 13 sight lines toward stars in seven distinctly different Galactic directions at distances ranging from 130 to 1500 pc, with most closer than 500 pc. These sight lines were particularly chosen for their wide range in physical conditions so as to search for evidence of density-dependent depletion variations in the gas-phase oxygen abundance as well as spatial variations.

2. OBSERVATIONS

The GHRS observations of the interstellar O I λ1356 absorption line toward the stars γ Cas, ϵ Per, δ Ori, ϵ Ori, 15 Mon, τ CMa, and γ Ara were obtained in 1995 October and November using the echelle A grating and the 2.″0 large science aperture. The detailed characteristics and in-flight performance of the GHRS instrument are discussed by Brandt et al. (1994) and Heap et al. (1995). The observations of each star consisted of multiple FP-split exposures centered near 1356 Å. An FP-split breaks up an exposure into four subexposures taken at slightly different grating positions so as to better characterize and minimize the impact of the GHRS Digicon detector's fixed pattern noise on the S/N ratio of the data. Each of these subexposures was sampled two or four times per Digicon diode (depending on the brightness of the star) at a velocity resolution of 3.5 km s^{-1}.

The data reduction procedure discussed in detail by Cardelli & Ebbets (1994) was utilized to maximize the S/N ratio of the O I spectra. Basically, this process involves four steps.

1. The subexposures comprising each FP-Split exposure are merged in diode space so as to create a template of the fixed pattern noise spectrum.
2. Each subexposure is divided by this noise template.
3. All of the rectified subexposures are aligned in wavelength space using the interstellar lines as a guide.
4. The aligned subexposures are summed to produce the net O I spectrum of each star.

As illustrated in Figure 1 for five of the stars in our echelle sample, the resulting continuum-flattened spectra reveal convincing detections of the interstellar O I λ1356 line in all seven sight lines. The measured S/N ratios of these spectra are all in the 400–600 range.

The GHRS spectra of λ Ori and ζ Per displayed in Figure 1 were obtained in 1994 February using the G160M grating and the 0.″25 small science aperture. These spectra were reduced in the same manner as the echelle data and are each characterized by a velocity resolution of 16 km s^{-1} and a S/N ratio of about 500. The measured equivalent widths of the interstellar O I λ1356 absorption in these spectra, as well as those in the echelle sight lines, are listed in Table 1. The uncertainties in these line strengths reflect the statistical and continuum placement errors summed in quadrature. Table 1 also includes the previously reported GHRS O I λ1356 measurements toward ι Ori and κ Ori (Meyer et al. 1994), ξ Per (Cardelli et al. 1991), and ζ Oph (Savage, Cardelli, & Sofia 1992).

The O I column densities listed in Table 1 were calculated from the λ1356 equivalent widths using the Zeippen, Seaton, & Morton (1977) oscillator strength of $f = 1.248 \times 10^{-6}$. Although the quoted uncertainty in this f-value is 15%, Sofia, Cardelli, & Savage (1994) have empirically verified that it is consistent with the better determined f-value appropriate for the O I λ1302 transition. In the cases of γ Cas, ϵ Per, δ Ori, ι Ori, ϵ Ori, κ Ori, 15 Mon, and τ CMa, the λ1356 absorption is weak enough for N(O I)

TABLE 1

GHRS Interstellar Oxygen Abundances

Star	N(H)[a] (cm^{-2})	$\log n_{\mathrm{H}}$[b] (cm^{-3})	$\log f(\mathrm{H}_2)$[c]	W_λ(1356)[d] (mÅ)	N(O I)[e] (cm^{-2})	10^6 O/H[f]
γ Cas	1.5 (0.2) $\times 10^{20}$	−0.60	< -2.36	1.1 (0.1)	5.4 (0.5) $\times 10^{16}$	367 (62)
ζ Per	1.6 (0.2) $\times 10^{21}$	0.11	−0.23	8.0 (0.5)	4.8 (0.6) $\times 10^{17}$	306 (49)
ϵ Per	3.3 (0.5) $\times 10^{20}$	−0.46	−0.69	2.1 (0.2)	1.0 (0.1) $\times 10^{17}$	316 (53)
ξ Per	1.9 (0.2) $\times 10^{21}$	0.18	−0.44	10.8 (1.3)	6.0 (0.8) $\times 10^{17}$	321 (53)
δ Ori	1.6 (0.2) $\times 10^{20}$	−0.87	−5.21	0.9 (0.1)	4.4 (0.5) $\times 10^{16}$	282 (46)
λ Ori	6.5 (1.2) $\times 10^{20}$	−0.38	−1.39	4.0 (0.5)	2.0 (0.3) $\times 10^{17}$	316 (71)
ι Ori	1.5 (0.2) $\times 10^{20}$	−1.02	−5.17	1.1 (0.2)	5.4 (1.0) $\times 10^{16}$	370 (81)
ϵ Ori	2.9 (0.4) $\times 10^{20}$	−0.73	−3.59	1.8 (0.2)	8.9 (1.0) $\times 10^{16}$	307 (55)
κ Ori	3.4 (0.3) $\times 10^{20}$	−0.66	−4.55	2.1 (0.2)	1.0 (0.1) $\times 10^{17}$	303 (40)
15 Mon	2.3 (0.4) $\times 10^{20}$	−0.97	−4.52	1.3 (0.3)	6.4 (1.5) $\times 10^{16}$	278 (81)
τ CMa	5.3 (0.4) $\times 10^{20}$	−0.95	−4.95	4.0 (0.3)	2.0 (0.2) $\times 10^{17}$	372 (40)
ζ Oph	1.4 (0.1) $\times 10^{21}$	0.52	−0.20	6.4 (0.6)	4.0 (0.4) $\times 10^{17}$	284 (32)
γ Ara	5.4 (0.6) $\times 10^{20}$	−0.59	−1.20	3.9 (0.2)	2.0 (0.2) $\times 10^{17}$	378 (51)

[a] $N(\mathrm{H}) = 2N(\mathrm{H}_2) + N(\mathrm{H\ I})$ is the total hydrogen column density ($\pm 1\ \sigma$) in the observed sight lines. These values reflect the H_2 column densities measured by Savage et al. 1977 and the weighted means of the Bohlin, Savage, & Drake 1978 and Diplas & Savage 1994 N(H I) data.

[b] Mean hydrogen sight line density is calculated from N(H) and the stellar distances.

[c] $f(\mathrm{H}_2) = 2N(\mathrm{H}_2)/N(\mathrm{H})$ is the fractional abundance of hydrogen nuclei in H_2 in the observed sight lines.

[d] Measured equivalent widths ($\pm 1\ \sigma$) of the O I 1355.598 Å absorption line.

[e] Derived O I column densities ($\pm 1\ \sigma$) in the observed sight lines. The ξ Per and ζ Oph values are taken from the analyses of Cardelli et al. 1991 and Savage, Cardelli, & Sofia 1992. The ζ Per, λ Ori, and γ Ara values are corrected for a slight amount of saturation using respective Gaussian b-values ($\pm 1\ \sigma$) of $2.0^{+2.0}_{-0.5}$, $5.0^{+\infty}_{-2.5}$, and $3.0^{+\infty}_{-1.5}$ km s^{-1}. The other sight lines are assumed to be optically thin in the O I λ1356 transition.

[f] Abundance of interstellar gas-phase oxygen ($\pm 1\ \sigma$) per 10^6 H atoms in the observed sight lines. The uncertainties reflect the propagated N(H) and N(O I) errors.

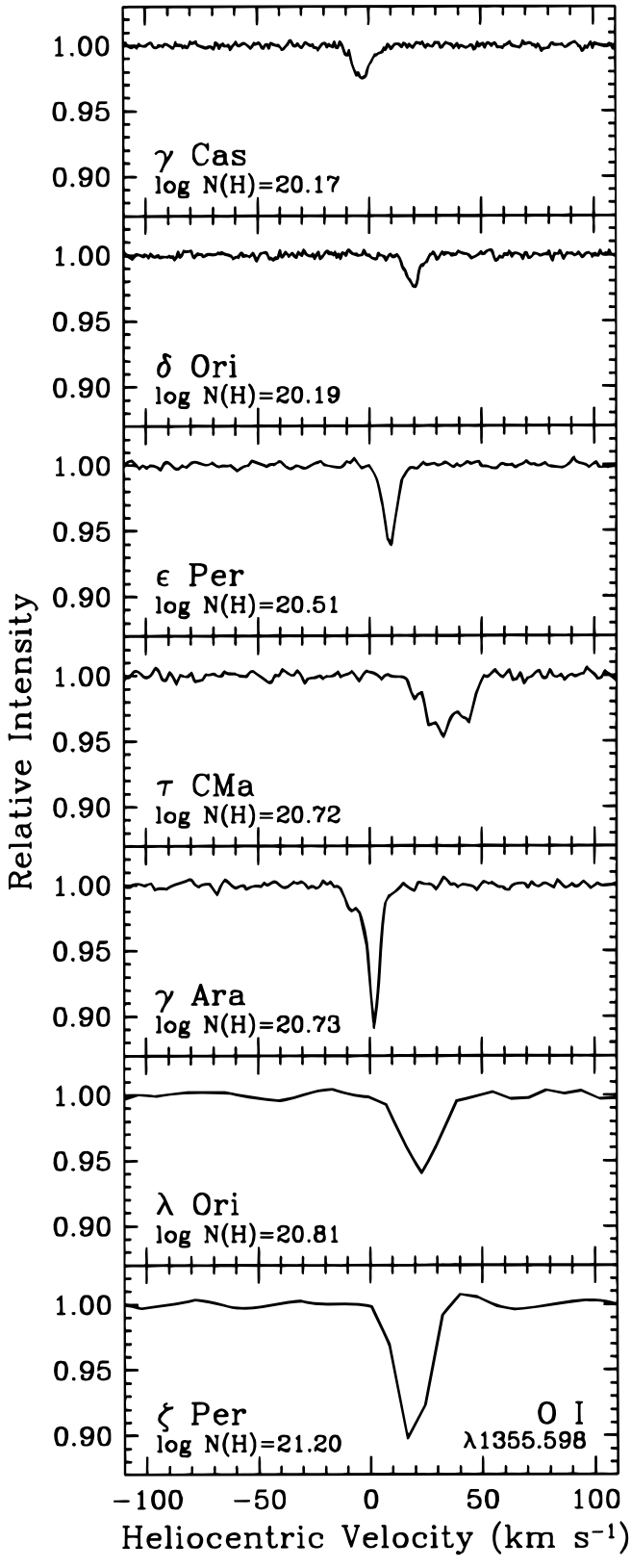

FIG. 1.—*HST* GHRS spectra of the interstellar O I λ1355.598 absorption line toward γ Cas, δ Ori, ε Per, τ CMa, and γ Ara at a velocity resolution of 3.5 km s^{-1} and toward λ Ori and ζ Per at a resolution of 16 km s^{-1}. The spectra are displayed from top to bottom in order of increasing total hydrogen column density in the observed sight lines. The measured S/N ratios of these spectra are all in the 400–600 range. The measured equivalent widths of the O I lines are listed in Table 1.

to be confidently derived under the assumption that the line is optically thin. In the cases of ζ Per, λ Ori, and γ Ara, a slight correction for saturation was applied using a Gaussian curve of growth with respective *b*-values of $2.0^{+2.0}_{-0.5}$, $5.0^{+\infty}_{-2.5}$, and $3.0^{+\infty}_{-1.5}$ km s^{-1}. These *b*-values were estimated from GHRS observations of the interstellar Mg II λλ1239.9,1240.4 doublet toward ζ Per, the Mg II and N I λλ1160,1161 (Meyer, Cardelli, & Sofia 1997) doublets toward λ Ori, and the O I λ1356 line width toward γ Ara. The resultant O I column densities for ζ Per, λ Ori, and γ Ara are 24%, 4%, and 6% greater than their weak-line limits, respectively. The N(O I) values corresponding to the slightly saturated λ1356 lines toward ξ Per and ζ Oph were taken from the detailed analyses of these sight lines by Cardelli et al. (1991) and Savage et al. (1992). The uncertainties in the O I column densities listed in Table 1 reflect the estimated errors in the λ1356 equivalent width measurements and the saturation corrections (where applied). These errors do not include the uncertainty in the λ1356 *f*-value because it would affect all of the column densities in the same way.

3. RESULTS

In order to put the GHRS oxygen results in perspective, it is instructive to compare and analyze them in concert with the best *Copernicus* satellite observations of the interstellar O I λ1356 line. Table 2 lists the 14 sight lines toward which the equivalent width of this line has been measured at the 4 σ level or better with *Copernicus* (Bohlin et al. 1983; Zeippen et al. 1977). Among the four sight lines in common between the GHRS and *Copernicus* samples, ζ Oph yields similar O I line strengths while the ε Per, λ Ori, and κ Ori lines are weaker in the more sensitive GHRS spectra. In deriving the *Copernicus* O I column densities listed in Table 2, ε Per and κ Ori were assumed to be optically thin while the λ Ori and ζ Oph lines were corrected for saturation in the same way as the GHRS data. Since the other sight lines in the *Copernicus* sample have appreciably stronger O I lines, saturation is more of a concern than in the general case of the GHRS sample. For these sight lines, saturation corrections were applied using a single-component Gaussian curve of growth and the *b*-value estimates listed in Table 2. The *b*-value estimates are based in part on *Copernicus* observations of interstellar Cl I and P II in these sight lines (Jenkins, Savage, & Spitzer 1986). The impact of the saturation corrections on N(O I) ranges from 12% over the weak-line limit for δ Sco to 68% for ρ Oph, and less than 30% for most of the other sight lines. The quoted errors in the derived O I column densities reflect the uncertainties in these corrections as well as those in the λ1356 line-strength measurements.

The total hydrogen column densities [N(H) = 2N(H$_2$) + N(H I)] listed in Tables 1 and 2 were determined in the same manner for each sight line in the GHRS and *Copernicus* samples. These values reflect the H$_2$ column densities measured by Savage et al. (1977) and the weighted means of the Bohlin, Savage, & Drake (1978) and Diplas & Savage (1994) N(H I) data. The uncertainties in the resulting oxygen abundances (per 10^6 H atoms) in Tables 1 and 2 reflect the propagated errors in both N(O I) and N(H). Taken together, the GHRS sight lines yield a weighted mean interstellar gas-phase oxygen abundance of 10^6 O/H = 319 ± 14, while the *Copernicus* data yield 10^6 O/H = 361 ± 20. Although the *Copernicus* mean is heavily weighted by the accurate

TABLE 2

Copernicus INTERSTELLAR OXYGEN ABUNDANCES

Star	$N(H)^a$ (cm^{-2})	$\log n_H{}^b$ (cm^{-3})	$\log f(H_2)^c$	$W_\lambda(1356)^d$ (mÅ)	b^e (km s^{-1})	$N(O\ I)^f$ (cm^{-2})	10^6 O/H^g
o Per	1.5 (0.2) × 10^{21}	0.08	−0.27	11.7 (2.4)	$2.0^{+2.0}_{-0.5}$	8.0 (1.8) × 10^{17}	535 (138)
ϵ Per.....	3.3 (0.5) × 10^{20}	−0.46	−0.69	3.5 (0.8)	...	1.7 (0.4) × 10^{17}	528 (140)
α Cam	1.3 (0.1) × 10^{21}	−0.46	−0.47	15.5 (3.3)	$5.0^{+\infty}_{-2.5}$	8.9 (2.1) × 10^{17}	690 (178)
λ Ori.....	6.5 (1.2) × 10^{20}	−0.38	−1.39	6.1 (1.3)	$5.0^{+\infty}_{-2.5}$	3.2 (0.7) × 10^{17}	492 (137)
κ Ori	3.4 (0.3) × 10^{20}	−0.66	−4.55	3.1 (0.3)	...	1.5 (0.2) × 10^{17}	450 (59)
1 Sco	1.6 (0.2) × 10^{21}	0.36	−1.66	13.3 (2.5)	$3.0^{+3.0}_{-1.0}$	8.3 (1.7) × 10^{17}	532 (126)
δ Sco	1.2 (0.2) × 10^{21}	0.39	−1.36	9.2 (0.8)	$4.0^{+\infty}_{-2.0}$	5.1 (0.7) × 10^{17}	422 (79)
β^1 Sco	1.3 (0.1) × 10^{21}	0.43	−0.99	7.8 (0.8)	$3.0^{+\infty}_{-1.0}$	4.4 (0.7) × 10^{17}	333 (56)
ω^1 Sco.....	1.7 (0.3) × 10^{21}	0.55	−0.88	11.9 (1.7)	$3.0^{+3.0}_{-1.0}$	7.2 (1.1) × 10^{17}	415 (97)
σ Sco	2.5 (0.3) × 10^{21}	0.73	−1.31	14.3 (1.6)	$2.0^{+2.0}_{-0.5}$	1.1 (0.3) × 10^{18}	432 (122)
ρ Oph	5.7 (0.7) × 10^{21}	1.06	−0.89	16.5 (3.3)	$2.0^{+2.0}_{-0.5}$	1.4 (0.5) × 10^{18}	239 (88)
χ Oph	2.4 (0.3) × 10^{21}	0.65	−0.44	26.0 (6.0)	$5.0^{+\infty}_{-2.0}$	1.7 (0.6) × 10^{18}	712 (253)
ζ Oph	1.4 (0.1) × 10^{21}	0.52	−0.20	6.6 (0.4)	$1.5^{+0.5}_{-0.3}$	4.1 (0.3) × 10^{17}	295 (29)
15 Sgr	1.8 (0.3) × 10^{21}	−0.48	−0.67	20.8 (4.3)	$5.0^{+\infty}_{-2.5}$	1.3 (0.4) × 10^{18}	717 (262)

[a] $N(H) = 2N(H_2) + N(H\ I)$ is the total hydrogen column density ($\pm 1\ \sigma$) in the observed sight lines. These values reflect the H_2 column densities measured by Savage et al. 1977 and the weighted means of the Bohlin, Savage, & Drake 1978 and Diplas & Savage 1994 $N(H\ I)$ data.

[b] Mean hydrogen sight line density is calculated from $N(H)$ and the stellar distances.

[c] $f(H_2) = 2N(H_2)/N(H)$ is the fractional abundance of hydrogen nuclei in H_2 in the observed sight lines.

[d] Measured equivalent widths ($\pm 1\ \sigma$) of the O I 1355.598 Å absorption line from Bohlin et al. 1983 and Zeippen, Seaton, & Morton 1977 (ζ Oph).

[e] Gaussian b-values ($\pm 1\ \sigma$) used to correct the O I λ1356 line for saturation in deriving $N(O\ I)$. The sight lines toward ϵ Per and κ Ori are assumed to be optically thin in this transition.

[f] Derived O I column densities ($\pm 1\ \sigma$) in the observed sight lines.

[g] Abundance of interstellar gas-phase oxygen ($\pm 1\ \sigma$) per 10^6 H atoms in the observed sight lines. The uncertainties reflect the propagated $N(H)$ and $N(O\ I)$ errors.

value toward ζ Oph, both samples are indicative of an interstellar gas-phase O abundance that is appreciably below the solar value of 10^6 O/H = 741 ± 130 (Grevesse & Noels 1993). The key improvement of the GHRS data over the *Copernicus* data is the greater accuracy of the individual GHRS measurements (especially of the weaker O I lines). In the GHRS data, the largest deviation of O/H from the mean value is 18% compared to a range in the *Copernicus* data of a factor of 3.

As reviewed by Jenkins (1987), the interstellar gas-phase abundances of many elements measured by *Copernicus* decrease as a function of the mean sight-line hydrogen density, $n_H = N(H)/r$, where r is the distance to the background star. These elemental depletions from the gas phase reflect both the growth of dust grains in denser clouds and grain destruction in more diffuse environments. Using the stellar distances listed in Diplas & Savage (1994), we have calculated n_H for each of the sight lines in our GHRS and *Copernicus* samples and plotted them against the corresponding oxygen abundances in Figure 3. As might be expected from Figure 2, there is no significant evidence of variations in the gas-phase O abundance as a function of n_H in either sample. Although the *Copernicus* data sample denser sight lines, the GHRS data pin down the oxygen gas abundance in the most diffuse clouds at a level that is completely consistent with the higher density cases. The absence of abundance variations as a function of n_H in the GHRS data suggests that there is negligible exchange between gas and dust in these diffuse sight lines and that the total (gas plus dust) abundance of oxygen must not vary significantly in the local ISM.

A better barometer of diffuse cloud conditions is the fractional abundance of molecular hydrogen, $f(H_2) = 2N(H_2)/N(H)$ (Cardelli 1994). Sight lines separate rather distinctly into groups with low and high $f(H_2)$ values due to the difference between UV transparent and H_2 self-shielding environments. Even for weakly depleted elements like Ge (Cardelli 1994) and Zn (Roth & Blades 1995; Sembach et al. 1995), the gas-phase abundances are higher in the low $f(H_2)$ group than in the high group, signifying both the presence of dust grains and changes in the elemental dust abundance due to interstellar grain growth and/or destruction. Figure 4 clearly shows that the interstellar gas-phase O abundances measured with GHRS are both well sampled as a function of $f(H_2)$ and exhibit no dependence on this parameter. Indeed, the mean abundance in the seven sight lines with $\log f(H_2) < -2.0$ (10^6 O/H = 325 ± 20) is essentially the same as that in the six sight lines with $\log f(H_2) > -2.0$ (10^6 O/H = 312 ± 19). Thus, any significant reservoir of interstellar oxygen in diffuse clouds other than the atomic gas must be resilient enough to survive in a variety of environments.

4. DISCUSSION

Under the traditional assumption that the *cosmic* elemental abundances reflect those in the solar system, the mean gas-phase abundance of interstellar oxygen measured by GHRS implies an O dust fraction of 10^6 O/H ≈ 420. However, it has been known for some time that an elemental inventory of the likely constituents of interstellar dust yields appreciably less solid-state oxygen than this inferred amount (Greenberg 1974; Meyer 1989). In particular, assuming various mixtures of oxygen-bearing grain compounds such as the silicates pyroxene [(Mg, Fe)SiO_3] and olivine [$(Mg, Fe)_2SiO_4$] and oxides like Fe_2O_3, it is difficult to increase the O dust fraction much beyond 10^6 O/H ≈ 180 (Cardelli et al. 1996), simply because the requisite metals are far less abundant than oxygen

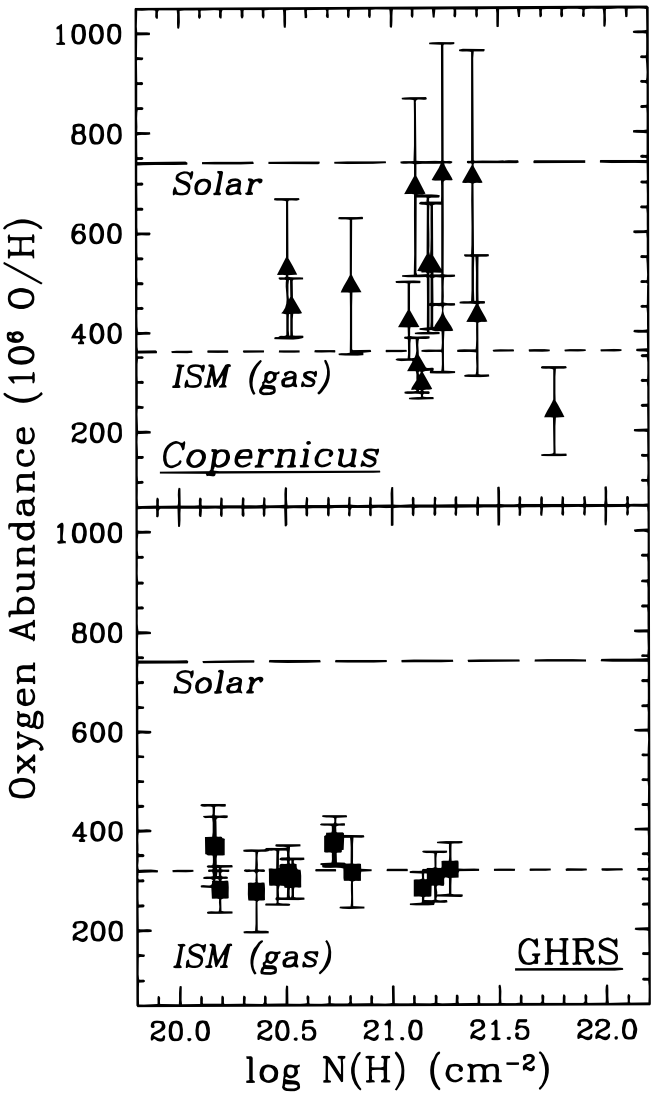

FIG. 2.—Interstellar oxygen abundances measured in our *Copernicus* and GHRS samples as a function of the logarithmic total hydrogen column density, $N(\mathrm{H}) = 2N(\mathrm{H}_2) + N(\mathrm{H\ I})$, in the observed sight lines. The short-dashed lines through the data points represent the respective *Copernicus* and GHRS weighted mean values (per 10^6 H atoms) of 10^6 O/H = 361 ± 20 and 10^6 O/H = 319 ± 14 for the interstellar gas-phase oxygen abundance. The long-dashed lines represent the Grevesse & Noels (1993) solar oxygen abundance (10^6 O/H = 741 ± 130).

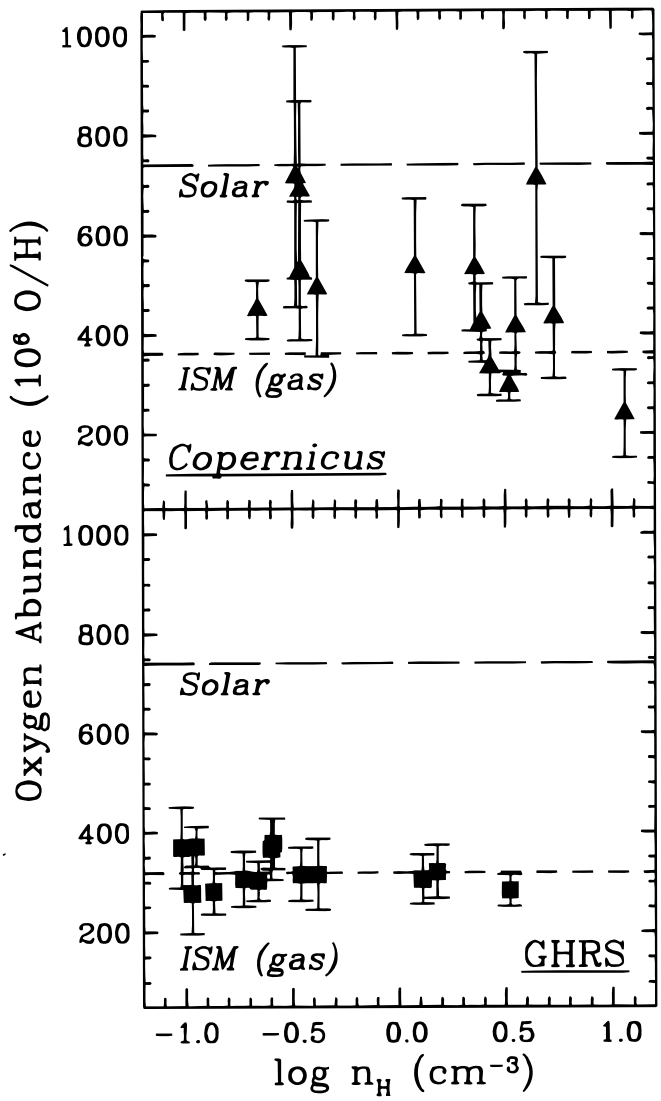

FIG. 3.—Interstellar oxygen abundances measured in our *Copernicus* and GHRS samples as a function of the logarithmic mean hydrogen density, $n_{\mathrm{H}} = N(\mathrm{H})/r$, in the observed sight lines. The short-dashed lines through the data points represent the respective *Copernicus* and GHRS weighted mean values (per 10^6 H atoms) of 10^6 O/H = 361 ± 20 and 10^6 O/H = 319 ± 14 for the interstellar gas-phase oxygen abundance. The long-dashed lines represent the Grevesse & Noels (1993) solar oxygen abundance (10^6 O/H = 741 ± 130).

$[(\mathrm{O{:}Si{:}Mg{:}Fe})_{\mathrm{solar}} \approx (24{:}1{:}1{:}1)]$. If these metals have total (gas plus dust) underabundances similar to that derived for oxygen, the implied O dust fraction would be 10^6 O/H ≈ 120, instead of 10^6 O/H ≈ 180. It would be hard to hide a significant amount in molecules like CO or O_2 in the diffuse sight lines observed by GHRS without leaving any trace of O abundance variations as a function of $f(H_2)$. For similar reasons, the "missing" oxygen is unlikely to be locked in icy grain mantles or ice grains (Greenberg 1974). Such carriers would also leave unmistakable signatures like the 3.07 μm O–H stretch "ice" feature that are not observed in diffuse sight lines (Whittet et al. 1988). Thus, unless there is some other resilient form of oxygen in the diffuse ISM, it appears clear from our GHRS observations that the *total* abundance of interstellar O is about two-thirds of the solar value. This result is consistent with the conclusions of the previous GHRS oxygen studies (Meyer et al. 1994; Cardelli et al. 1996) that used subsets of the complete sight line sample presented here.

The possibility that the interstellar oxygen measurements are sampling an overall deficit in local ISM elemental abundances has been enhanced by recent GHRS observations of interstellar krypton. Based on measurements in 10 sight lines, Cardelli & Meyer (1997) find a mean interstellar gas-phase Kr abundance that is about 60% of the solar system abundance. Since Kr, as a noble gas, should not be depleted much into dust grains, this gas-phase abundance reflects a true interstellar deficit similar to what we find for oxygen. Furthermore, the abundance of krypton, like oxygen, is remarkably homogeneous from sight line to sight line independent of diffuse cloud conditions. This homogeneity is reflected in Figure 5, where we plot the interstellar gas-phase O/Kr abundance ratio as a function of $f(H_2)$ for the GHRS sight lines in common between this study and that of

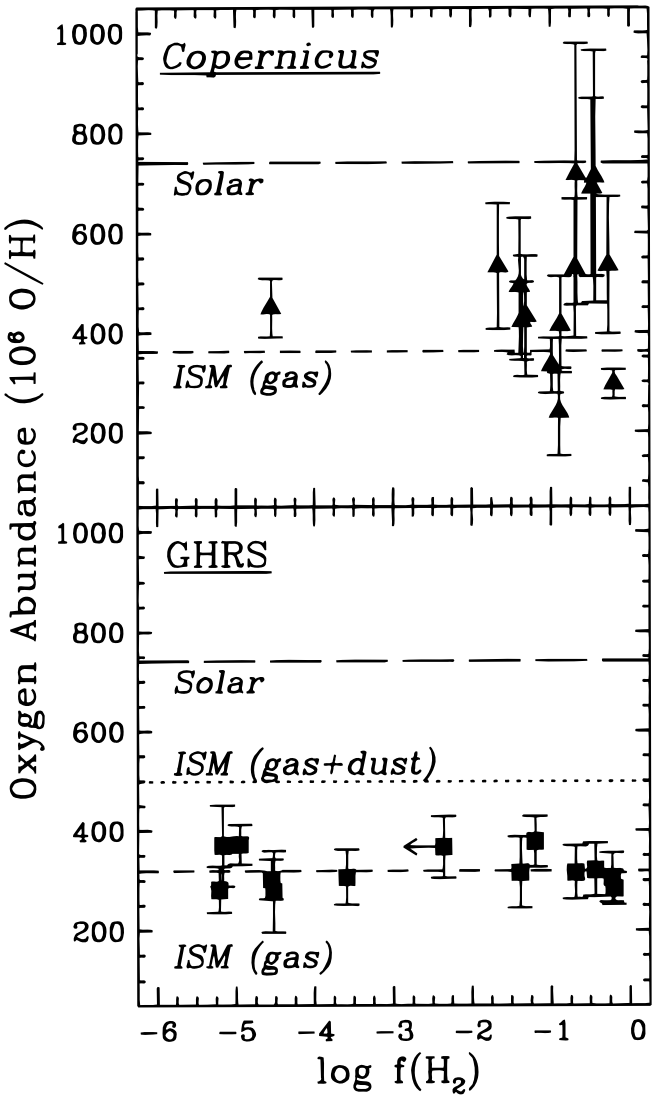

FIG. 4.—Interstellar oxygen abundances measured in our *Copernicus* and GHRS samples as a function of the logarithmic fraction of hydrogen in molecular form, $f(H_2) = 2N(H_2)/N(H)$, in the observed sight lines. The short-dashed lines through the data points represent the respective *Copernicus* and GHRS weighted mean values (per 10^6 H atoms) of 10^6 O/H $= 361 \pm 20$ and 10^6 O/H $= 319 \pm 14$ for the interstellar gas-phase oxygen abundance. The *dotted line* above the GHRS data points at 10^6 O/H ≈ 500 reflects the *total* (gas plus dust) GHRS interstellar oxygen abundance, after an allowance is made for the O tied up in dust grains. This value is about two-thirds of the Grevesse & Noels (1993) solar oxygen abundance (10^6 O/H $= 741 \pm 130$) denoted by the long-dashed lines in the figure.

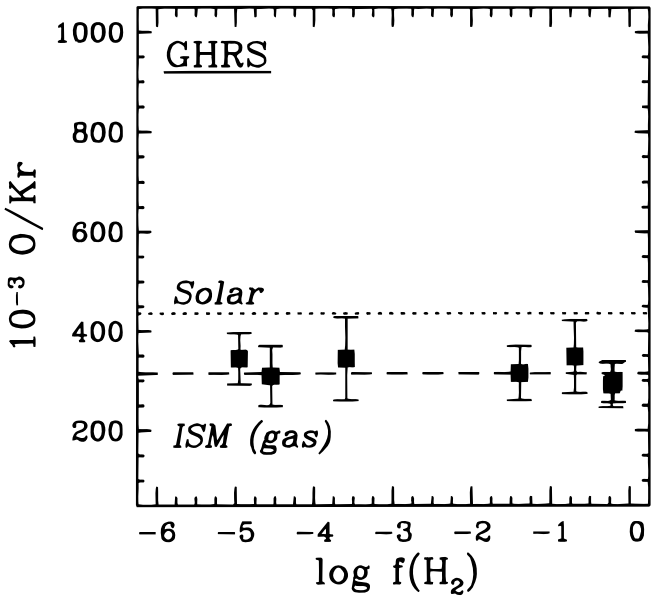

FIG. 5.—Interstellar gas-phase O/Kr abundance ratio measured with GHRS as a function of the logarithmic fraction of hydrogen in molecular form, $f(H_2) = 2N(H_2)/N(H)$, in the seven observed sight lines with both O (this paper) and Kr (Cardelli & Meyer 1997) data. The dashed line among the data points reflects their weighted mean value of 10^{-3} O/Kr $= 314 \pm 20$. After accounting for the O tied up in dust grains, this ratio comes close to the solar value of 10^{-3} O/Kr $= 436 \pm 108$ (Anders & Grevesse 1989; Grevesse & Noels 1993).

Cardelli & Meyer (1997). The current data are consistent with a picture where the abundances of all of the elements in the local ISM are generally about 2/3 of their solar system values (Snow & Witt 1995, 1996).

The interstellar abundance deficit suggested by the GHRS observations of O and Kr fortifies the results of nearby B star measurements of the current epoch abundances of O and other elements (Gies & Lambert 1992; Kilian 1992; Cunha & Lambert 1994; Kilian et al. 1994). As discussed earlier, these studies yield median B star CNO abundances that are also about two-thirds of the solar values. The implication of this result is that something unusual happened to either the Sun or the local ISM in the context of standard models of Galactic chemical evolution (Audouze & Tinsley 1976; Timmes et al. 1995).

The ± 0.05 dex spread in the interstellar oxygen abundances is appreciably less than the ± 0.2 dex oxygen spread in Orion B stars (Cunha & Lambert 1994) and the ± 0.25 dex Fe abundance spread in the solar-like star sample of Edvardsson et al. (1993). If one believes that these stellar abundance spreads are real and not due to observational error, the question arises as to how to make stars with such large abundance variations out of a very well mixed ISM. The GHRS data certainly make it difficult now to explain the solar anomaly simply as the result of a typical ISM abundance fluctuation. There are three models to explain why the ISM has a lower oxygen abundance than does the Sun.

1. Based on isotopic anomalies involving ^{26}Al and other elements in meteorites and cosmic rays, the idea that the early solar system was chemically enriched by a local supernova explosion has long been popular (Reeves 1978; Lee 1979; Olive & Schramm 1982). At first glance, this idea would seem to be a reasonable explanation for the overabundance of oxygen in the Sun. If the solar system originated in a molecular cloud with active OB star formation, a first generation of massive stars could have evolved quickly and enriched the gas in heavy elements such as oxygen, that would later be incorporated in the Sun. Cunha & Lambert (1994) have found evidence of such a process in the Orion OB association where elements such as oxygen, which is produced in abundance by Type II supernovae, exhibit larger abundance spreads in the B stars than do elements like nitrogen. In the context of the Edvardsson et al. (1993) study of solar-like stars, if this kind of cloud self-enrichment process were common, it could also explain the stellar Fe

abundance spread as well as the Sun's position near the top. Yet our GHRS data indicate that the ISM abundance inhomogeneities produced by any such process must be quickly damped out. In particular, our five GHRS Orion sight lines yield a spread of only ± 0.05 dex in their interstellar oxygen gas abundances and a mean value of 10^6 O/H $= 305 \pm 24$, which is completely consistent with that of the other GHRS sight lines (10^6 O/H $= 325 \pm 17$). Even if this mixing problem can be accommodated through Galactic hydrodynamical processes (Roy & Kunth 1995), the supernova enrichment hypothesis still faces the challenge of creating similar overabundances for a variety of elements in the Sun. For example, in addition to O and Kr, the early GHRS results on interstellar nitrogen also yield a two-thirds solar abundance for this element (Cardelli et al. 1996). Given the steep relative yield of O to N in Type II supernovae (Olive & Schramm 1982), as compared to their present-day interstellar abundances, it is difficult to understand how one or more such explosions could have produced similar overabundances of these two elements, let alone others, in the protosolar nebula.

2. As discussed by Meyer et al. (1994) and Roy & Kunth (1995), another approach to understanding the underabundance of interstellar oxygen is to invoke a recent infall of metal-poor extragalactic gas in the local Milky Way. The idea of infall, whether gradual or episodic, has long been recognized as a potentially important component of Galactic chemical evolution (Audouze & Tinsley 1976; Mayor & Vigroux 1981; Pitts & Tayler 1989; Chiappini, Matteucci, & Gratton 1997). Recent observations of high-velocity gas in the Galactic halo indicate that at least some of these infalling clouds have metallicities as low as 10% of the solar value (Kunth et al. 1994; Lu, Savage, & Sembach 1994). Comeron & Torra (1994) have suggested that the impact of a $\approx 10^6\ M_\odot$ extragalactic cloud with the local Milky Way some 10^8 years ago could explain the origin and characteristics of the nearby early-type stars and molecular clouds that constitute the Gould Belt. In terms of the resultant metallicity of the mixed gas, such a collision could also have diluted the heavy-element abundances in the local ISM below their solar values. Since this dilution would affect all of the elements in the same way, the similar interstellar underabundances observed for O and Kr could easily be explained through an infall model. Conversely, such a model would have serious problems if any element was found not to exhibit this underabundant pattern. Sulfur is a potential candidate to break this pattern since Fitzpatrick & Spitzer (1997) have measured near-solar interstellar gas-phase S abundances toward three stars with high-quality GHRS data. However, these abundances are quite uncertain because of the considerable saturation of the S II $\lambda\lambda$1251,1254,1260 absorption lines and the likely possibility that a significant fraction of the S II (which has an ionization potential of 23.3 eV) originates in H II regions.

Another prediction of the local infall hypothesis would be that the abundances just beyond the Gould Belt should be closer to the solar values. In terms of the B stars within a kiloparsec or so, the data are generally inconclusive on this point with O abundance spreads of about ± 0.2 dex and no systematic variations found (Gehren et al. 1985; Fitzsimmons, Dufton, & Rolleston 1992; Kilian-Montenbruck, Gehren, & Nissen 1994; Kaufer et al. 1994; Smartt 1996). However, in a comprehensive study of B stars over a large range of Galactocentric distance ($6 \leq R_g \leq 18$ kpc), Smartt & Rolleston (1997) find an oxygen abundance gradient of -0.07 ± 0.01 dex kpc^{-1} that they claim should be representative of the present-day Galactic ISM. This large-scale gradient is consistent with that measured for oxygen in H II regions (Shaver et al. 1983; Simpson et al. 1995; Afflerbach et al. 1996) and planetary nebulae (Maciel & Koppen 1994). Unfortunately, the small-scale scatter in all of these gradient measures is too large to shed much light on the local infall hypothesis.

3. Wielen, Fuchs, & Dettbarn (1996) suggest that the Sun actually formed in the more metal-rich ISM at a Galactocentric distance of $R_g = 6.6 \pm 0.9$ kpc and has migrated over the past 4.6 Gyr to its current distance of $R_g = 8.5$ kpc. This scenario is predicated on a very smooth ISM metallicity gradient and a process of radial stellar diffusion that would lead to both the Sun's enhanced Fe metallicity and the observed ± 0.25 dex spread in the Fe abundances of nearby solar-like stars (Edvardsson et al. 1993). In terms of our GHRS interstellar O abundances, this idea is attractive because it could explain both the solar oxygen overabundance and how such a well-mixed local ISM could coexist with the much greater metallicity spreads of local stellar populations. The key challenge for the Wielen et al. scenario is working out the basic mechanism through which the stellar orbits can appreciably migrate radially. Furthermore, based on the ± 0.2 dex spread of the O abundances in the Orion B stars (Cunha & Lambert 1994), it is clear that stellar diffusion cannot be responsible for every large stellar abundance spread.

All three of these models are subject to future observational tests. If the abundances of all of the elements in the local ISM are two-thirds solar, then the model that the Sun was enriched by a local supernova is untenable. Accurate measurements of interstellar abundances at distances greater than 1 kpc will allow us to test models that predict spatial variations of these quantities.

This work was supported by NASA through grant NAG5-2178 to UCLA.

REFERENCES

Afflerbach, A., Churchwell, E., Acord, J. M., Hofner, P., Kurtz, S., & DePree, C. G. 1996, ApJS, 106, 423
Anders, E., & Grevesse, N. 1989, Geochim. Cosmochim. Acta, 53, 197
Audouze, J., & Tinsley, B. M. 1976, ARA&A, 14, 43
Baldwin, J. A., Ferland, G. J., Martin, P. G., Corbin, M. R., Cota, S. A., Peterson, B. M., & Slettebak, A. 1991, ApJ, 374, 580
Bohlin, R. C., Hill, J. K., Jenkins, E. B., Savage, B. D., Snow, T. P., Spitzer, L., & York, D. G. 1983, ApJS, 51, 277
Bohlin, R. C., Savage, B. D., & Drake, J. F. 1978, ApJ, 224, 132
Brandt, J., et al. 1994, PASP, 106, 890
Cardelli, J. A. 1994, Science, 265, 209
Cardelli, J. A., & Ebbets, D. C. 1994, in Calibrating *Hubble Space Telescope*, ed. J. C. Blades & S. J. Osmer (Baltimore: STScI), 322
Cardelli, J. A., & Meyer, D. M. 1997, ApJ, 477, L57
Cardelli, J. A., Meyer, D. M., Jura, M., & Savage, B. D. 1996, ApJ, 467, 334
Cardelli, J. A., Savage, B. D., Bruhweiler, F. C., Smith, A. M., Ebbets, D. C., Sembach, K. R., & Sofia, U. J. 1991, ApJ, 377, L57
Chiappini, C., Matteucci, F., & Gratton, R. 1997, ApJ, 477, 765
Comeron, F., & Torra, J. E. 1994, A&A, 281, 35
Cunha, K., & Lambert, D. L. 1994, ApJ, 426, 170
Diplas, A., & Savage, B. D. 1994, ApJS, 93, 211
Edvardsson, B., Andersen, J., Gustafsson, B., Lambert, D. L., Nissen, P. E., & Tomkin, J. 1993, A&A, 275, 101
Fitzpatrick, E. L., & Spitzer, L. 1997, ApJ, 475, 623
Fitzsimmons, A., Dufton, P. L., & Rolleston, W. R. J. 1992, MNRAS, 259, 489

Gehren, T., Nissen, P. E., Kudritzki, R. P., & Butler, K. 1985, in Proc. ESO Workshop on Production and Distribution of CNO Elements (Garching: ESO), 171
Gies, D. R., & Lambert, D. L. 1992, ApJ, 387, 673
Greenberg, J. M. 1974, ApJ, 189, L81
Grevesse, N., & Noels, A. 1993, in Origin and Evolution of the Elements, ed. N. Prantzos, E. Vangioni-Flam, & M. Casse (Cambridge: Cambridge Univ. Press), 15
Heap, S. R., et al. 1995, PASP, 107, 871
Jenkins, E. B. 1987, in Interstellar Processes, ed. D. J. Hollenbach & H. A. Thronson (Dordrecht: Reidel), 533
Jenkins, E. B., Savage, B. D., & Spitzer, L. 1986, ApJ, 301, 355
Kaufer, A., Szeifert, T., Krenzin, R., Baschek, B., & Wolf, B. 1994, A&A, 289, 740
Keenan, F. P., Hibbert, A., & Dufton, P. L. 1985, A&A, 147, 89
Kilian, J. 1992, A&A, 262, 171
Kilian, J., Montenbruck, O., & Nissen, P. E. 1994, A&A, 284, 437
Kilian-Montenbruck, J., Gehren, T., & Nissen, P. E. 1994, A&A, 291, 757
Kunth, D., Lequeux, J., Sargent, W. L. W., & Viallefond, F. 1994, A&A, 282, 709
Lee, T. 1979, Rev. Geophys. Space Phys., 17, 1591
Lu, L., Savage, B. D., & Sembach, K. R. 1994, ApJ, 437, L119
Maciel, W. J., & Koppen, J. 1994, A&A, 282, 43
Mayor, M., & Vigroux, L. 1981, A&A, 98, 1
Meyer, D. M., Cardelli, J. A., & Sofia, U. J. 1997, ApJ, 490, L103
Meyer, D. M., Jura, M., Hawkins, I., & Cardelli, J. A. 1994, ApJ, 437, L59
Meyer, J. P. 1989, in Cosmic Abundances of Matter, ed. J. C. Waddington (New York: AIP), 245
Olive, K. A., & Schramm, D. N. 1982, ApJ, 257, 276
Osterbrock, D. E., Tran, H. D., & Veilleux, S. 1992, ApJ, 389, 305
Peimbert, M., Storey, P. J., & Torres-Peimbert 1993, ApJ, 414, 626
Pitts, E., & Tayler, R. J. 1989, MNRAS, 240, 373
Reeves, H. 1978, in Protostars and Planets, ed. T. Gehrels (Tucson: Univ. Arizona Press), 399
Roth, K. C., & Blades, J. C. 1995, ApJ, 445, L95
Roy, J. R., & Kunth, D. 1995, A&A, 295, 432
Rubin, R. H., Simpson, J. P., Haas, M. R., & Erickson, E. F. 1991, ApJ, 374, 564
Savage, B. D., Bohlin, R. C., Drake, J. F., & Budich, W. 1977, ApJ, 216, 291
Savage, B. D., Cardelli, J. A., & Sofia, U. J. 1992, ApJ, 401, 706
Savage, B. D., & Sembach, K. R. 1996, ARA&A, 34, 279
Sembach, K. R., Steidel, C. C., Macke, R. J., & Meyer, D. M. 1995, ApJ, 445, L27
Shaver, P. A., McGee, R. X., Newton, M. P., Danks, A. C., & Pottasch, S. R. 1983, MNRAS, 204, 53
Simpson, J. P., Colgan, S. W. J., Rubin, R. H., Erickson, E. F., & Hass, M. R. 1995, ApJ, 444, 721
Smartt, S. J. 1996, Ph.D. thesis, Queen's Univ. of Belfast
Smartt, S. J., & Rolleston, W. R. J. 1997, ApJ, 481, L47
Snow, T. P., & Witt, A. N. 1995, Science, 270, 1455
———. 1996, ApJ, 468, L65
Sofia, U. J., Cardelli, J. A., & Savage, B. D. 1994, ApJ, 430, 650
Timmes, F. X., Woosley, S. E., & Weaver, T. A. 1995, ApJS, 98, 617
Whittet, D. C. B., Bode, M. F., Longmore, A. J., Adamson, A. J., McFadzean, A. D., Aiken, D. K., & Roche, P. F. 1988, MNRAS, 233, 321
Wielen, R., Fuchs, B., & Dettbarn, C. 1996, A&A, 314, 438
York, D. G., Spitzer, L., Bohlin, R. C., Hill, J., Jenkins, E. B., Savage, B. D., & Snow, T. P. 1983, ApJ, 266, L55
Zeippen, C. J., Seaton, M. J., & Morton, D. C. 1977, MNRAS, 181, 527